JOURNAL OF THE MECHANICAL BEHAVIOR OF BIOMEDICAL MATERIALS 29 (2014) 403–416

Available online at www.sciencedirect.com

ScienceDirect

www.elsevier.com/locate/jmbbm


Research Paper

# Correlation between the mechanical and histological properties of liver tissue

Berkay Yarpuzlu[a], Mehmet Ayyildiz[a], Olgu Enis Tok[b], Ranan Gulhan Aktas[b], Cagatay Basdogan[a,*]

[a]College of Engineering, Koç University, Istanbul 34450, Turkey
[b]School of Medicine, Koç University, Istanbul, Turkey

ARTICLE INFO

*Article history:*
Received 14 June 2013
Received in revised form
11 September 2013
Accepted 13 September 2013
Available online 10 October 2013

*Keywords:*
Bovine liver
Material characterization
Hyperelasticity
Viscoelasticity
Fracture toughness
Finite element modeling
Histology

ABSTRACT

In order to gain further insight into the mechanisms of tissue damage during the progression of liver diseases as well as the liver preservation for transplantation, an improved understanding of the relation between the mechanical and histological properties of liver is necessary. We suggest that this relation can only be established truly if the changes in the states of those properties are investigated dynamically as a function of post mortem time. In this regard, we first perform mechanical characterization experiments on three bovine livers to investigate the changes in gross mechanical properties (stiffness, viscosity, and fracture toughness) for the preservation periods of 5, 11, 17, 29, 41 and 53 h after harvesting. Then, the histological examination is performed on the samples taken from the same livers to investigate the changes in apoptotic cell count, collagen accumulation, sinusoidal dilatation, and glycogen deposition as a function of the same preservation periods. Finally, the correlation between the mechanical and histological properties is investigated via the Spearman's Rank-Order Correlation method. The results of our study show that stiffness, viscosity, and fracture toughness of bovine liver increase as the preservation period is increased. These macroscopic changes are very strongly correlated with the increase in collagen accumulation and decrease in deposited glycogen level at the microscopic level. Also, we observe that the largest changes in mechanical and histological properties occur after the first 11–17 h of preservation.



## 1. Introduction

Liver plays a major role in metabolism and acts as a source of energy for the body by storing glycogen. In addition, working with other systems and organs, it is responsible for several important functions such as storing iron, detoxifying harmful substances, maintaining the hormonal balance, producing bile to help with the digestion, regulating blood clotting, and producing immune factors to fight infections. However, it is also prone to many diseases such as hepatitis, fatty liver, cirrhosis, and cancer. Liver fibrosis (scarring) is associated with major alterations in both the quantity and composition of extracellular matrix (ECM). A fibrotic liver contains more ECM than a healthy one, including fibronectin, undulin, elastin, laminin, hyaluronan, proteoglycans, and especially collagen fibers (Battaler and Brenner, 2005). In fact, liver

*Corresponding author. Tel.: +90 212 338 1721; fax: +90 212 338 1548.
E-mail address: cbasdogan@ku.edu.tr (C. Basdogan).

1751-6161/$ - see front matter © 2013 Elsevier Ltd. All rights reserved.
http://dx.doi.org/10.1016/j.jmbbm.2013.09.016

fibrosis is considered as the net result of the imbalance between the collagen fiber synthesis and decomposition. When fiber synthesis is very active and the decomposition is suppressed, then apoptosis is induced and liver fibrosis advances. If the progression of disease becomes severe, then liver failure occurs. Currently, the progression of liver disease is quantified by a liver biopsy, followed by a histological examination under a light microscope (Cui et al., 2010; Rockey et al., 2009). Specific staining of ECM fibers is used to quantify the degree of liver fibrosis using computer-guided morphometric analysis. The liver biopsy is an invasive procedure with many disadvantages including the possibility of causing bleeding, allergic reactions, and renal failure on the patient. Additionally, the operation can be risky for patients who have blood disorders and congestive heart failures. Therefore, non-invasive measurement and diagnosis of liver diseases is desirable. One of the challenges in this regard is to establish a correlation between the material properties of liver measured non-invasively and its histological states. Medical imaging techniques based on transient ultrasound elastography, called FibroScan (Sandrin et al., 2003; Ziol et al., 2005) and Magnetic Resonance Elastography, MRE, (Manduca et al., 2001; Huwart et al., 2006) have been utilized to quantify liver fibrosis non-invasively. In both approaches, the material properties of liver measured at a certain frequency of stimulation have been correlated with the fibrosis scores obtained from large patient groups for validation. FibroScan and MRE measurements have demonstrated the increase in elastic modulus of liver tissue with an increase in fibrosis level. These measurements are performed externally without having any direct contact with the actual liver tissue. In addition to the medical imaging techniques, mechanical characterization techniques have been also utilized to correlate material properties of liver with fibrosis levels. Mazza et al. (2007) conducted in vivo and ex vivo experiments with 10 human subjects having some liver pathology. Static mechanical properties were measured invasively on diseased liver segments using an aspiration device and fibrotic tissue is found three times stiffer than the normal tissue. Ozcan et al. (2011) performed invasive experiments with an impact hammer on 15 human livers, harvested from the patients having some form of liver disease, to investigate the frequency-dependent dynamic material properties of liver tissue as a function of liver fibrosis. They also observed an increase in elastic (storage) modulus of human liver as a function of increase in fibrosis level, characterized by histological scoring. Leal-Egaña et al. (2012) correlated the stiffness of the human liver cells with fibrosis level. The presence of live and dead cells, and the size distributions were measured. They suggested that tuning liver stiffness could play an essential role in the control of primary liver tumors. Lake and Barocas (2012) investigated the collagen alignment on the mechanical and structural behavior of liver tissue subjected to compression. They observed that there is no significant difference between the mechanical peak responses, but there is a significant difference between stress relaxation responses of samples with different alignments.

In the studies discussed above, the mechanical properties have been correlated with fibrosis scores to diagnose a disease or its severity. However, the fibrosis scores utilized in those studies do not really represent measurements of a continuous variable, but rather a degree of severity at a certain state of disease. As a result, the dynamic relation between the mechanical and histological properties has not been established. Moreover, the terminology used in histological examination is not precise; the scoring mostly relies on qualitative descriptions rather than quantitative measurements. There are problems in obtaining reproducible scores, since the process heavily relies on the expertise of the examiner (Shiha and Zalata, 2011). In this paper, we propose quantitative techniques to investigate the relation between mechanical and histological properties of liver to gain further insight into the mechanisms of tissue damage during the progression of liver diseases.

Another area where this insight can be helpful is the liver transplantation. The transplantation is the only treatment available today for severe liver failure. In this process, the diseased liver is replaced with a healthy one harvested from a donor. The liver harvested from a donor must be well preserved and then transported to the recipient immediately. Along this process, tissue damage occurs in the liver due to the drop in its temperature (hypothermia) and insufficient supply of blood to its vessels (ischemia). In order to preserve the liver during transportation, it is placed in a bag containing a chemical solution covered with ice. While the chemical solutions suggested in the literature for preserving a liver differ in components, they all aim to delay cell death (apoptosis), which is inevitable (Guibert et al., 2011). During apoptosis, morphological changes in ECM structure and cell shape such as shrinkage and bulging are observed. Additionally, due to the ischemia, the endothelial cells start to die, triggering hepatic sinusoidal dilatation. The glycogen stored in the tissue is consumed by the living cells to obtain additional energy during this preservation period, resulting in a decrease in the glycogen level of tissue (Corps et al., 2009; Jain et al., 2004; Natori et al., 1999). All these changes in histology of liver can be detected via specialized stains and quantified by image processing tools under light microscope. However, there is no consensus among the surgeons and experts on how long the preservation period must be. Again, investigating the changes in mechanical and histological properties as a function of preservation time and the correlation between them can provide insight into (a) how long a liver can be preserved before it is transplanted to a recipient and (b) how to design the chemical solutions to elongate the preservation period.

In summary, although there are studies available about the mechanical and histological properties of liver separately, the number of studies in the literature investigating the relation between them is very limited. Moreover, in the existing studies, no attention has been paid to the '*dynamical*' changes in those properties as a function of elapsed time. In this study, we investigate the correlation between the changes in gross mechanical and histological properties of liver tissue as a function of preservation time. This approach is inspired by the dynamical systems theory, where the continuous behavior of a complex dynamical system is investigated as a function of time.

Mechanical characterization experiments and histological examination are performed on three bovine livers 5, 11, 17, 29, 41 and 53 h after harvesting. First, static indentation and ramp-and-hold experiments are performed on each liver with

a cylindrical probe having a hemispherical tip to estimate its hyper-viscoelastic material properties for different preservation periods. Then, needle insertion experiments are performed on the same liver with a sharp probe to estimate its fracture toughness. A finite element (FE) model of bovine liver developed in ANSYS and an inverse FE analysis is performed on the model to estimate the material properties of each liver (Samur et al., 2007; Gokgol et al., 2012). To investigate the histological properties, the tissue samples taken from the same livers are stained with different methods. They are labeled with TUNEL apoptosis detection kit to count the number of apoptotic cells. Masson's trichrome stain is used to measure the amount of collagen accumulation. Glycogen deposition is investigated with Periodic Acid Schiff reagent. Sinusoidal dilatation, another histopathologic change in liver, is examined with Hematoxylene and Eosin stain. Following the measurement of the mechanical and histological properties as a function of the preservation time, the correlation between them is investigated via the Spearman's Rank-Order Correlation method. Moreover, a sensitivity analysis is performed on the mechanical and histological properties to determine the upper limit for the preservation period based on the largest changes in the properties.

## 2. Materials and methods

### 2.1. *Preparation of livers for mechanical characterization*

In this study, experiments are performed on three bovine livers to investigate the relation between the mechanical and the histological properties of liver tissue as a function of post-mortem time. The livers are preserved in Lactated Ringer's solution at +4 °C immediately after the harvesting. The right lobe of each liver is detached from the whole liver with the help of a sharp knife and all the experiments are performed on this lobe (Fig. 1). The transfer of the livers from the slaughterhouse to our laboratory took 4 h and the preparation for the experiments took another hour following the transfer. Three sets of mechanical experiments (static indentation, ramp-and-hold, and needle insertion) are performed on each liver 5, 11, 17, 29, 41 and 53 h after harvesting using the

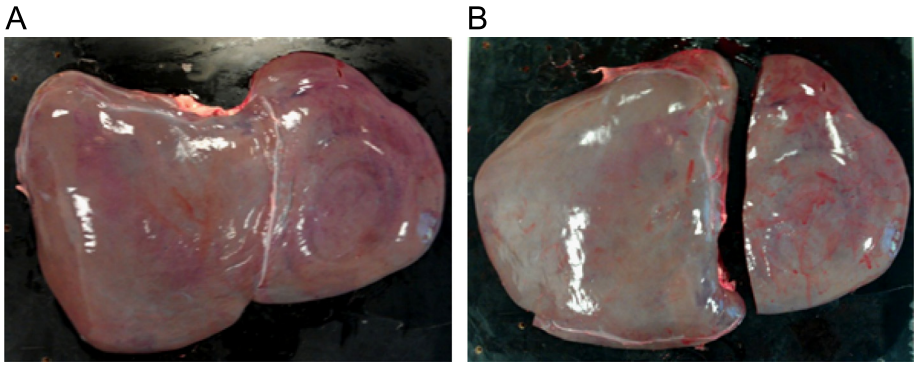


**Fig. 1 – (A) One of the bovine livers tested in our study and (B) its separated right lobe.**

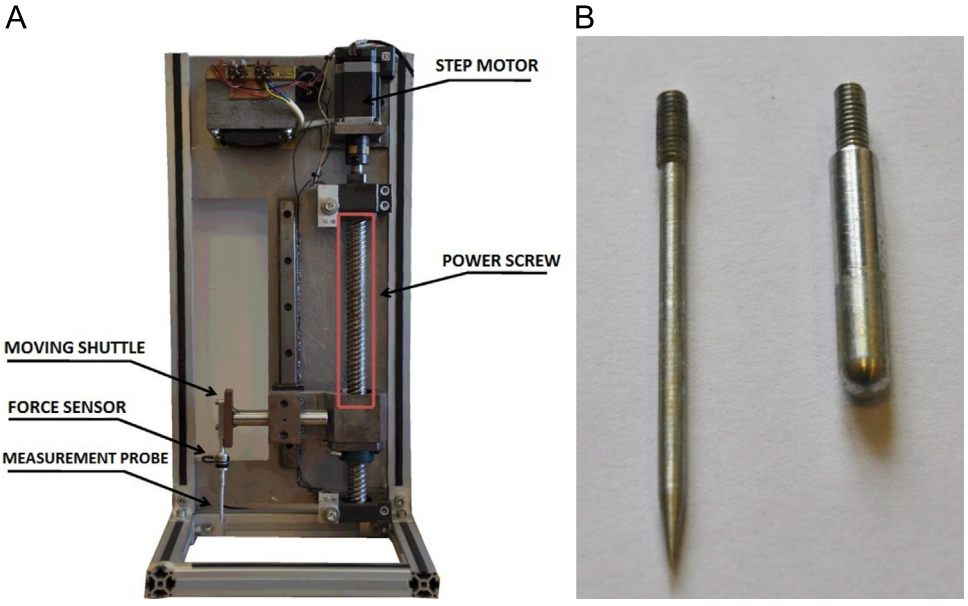


**Fig. 2 – (A) Our set-up for conducting mechanical characterization experiments. (B) The needle (diameter=3 mm) and the cylindrical probe (diameter=6 mm) used for the mechanical characterization experiments.**

experimental setup developed in our laboratory (Ocal et al., 2010). This setup consists of a step motor, a power screw, a moving nut on the power screw, a probe/needle on the nut, and a force sensor (Fig. 2A). All experiments were performed in the central region of the right lobe of each liver. Attention is paid to stay away from the edges of the liver to reduce the boundary effects. Each experiment was repeated five times at different locations in close proximity.

### 2.2. Static indentation experiments

Static indentation experiments are performed on the livers to investigate their strain-dependent hyperelastic material properties (Fig. 3). Each liver is compressed to 20 mm depth with the aid of a cylindrical probe (Fig. 2B) at a slow rate of 0.5 mm/s to minimize the dynamic effects. The force response of liver tissue is measured as a function of the compression depth.

### 2.3. Ramp-and-hold experiments

Ramp-and-hold experiments are performed on the livers to investigate their time-dependent viscoelastic material properties. First, each liver is compressed to 20 mm depth at a rate of 48 mm/s using the cylindrical probe. Then, the probe is held at that position for 600 s and the force response of the liver tissue is measured as a function of relaxation time.

### 2.4. Needle insertion experiments

Needle insertion experiments are performed on the livers with a sharp needle to estimate their fracture toughness. The needle is penetrated into 20 mm depth with a rate of 3 mm/s and the force response is measured as a function of the penetration depth. Following a brief period of relaxation, the needle is retracted from the liver, only to be inserted once more into the same hole to measure the force response again. The fracture toughness is estimated from these two consecutive measurements using the energy-based fracture mechanics approach (Gokgol et al., 2012).

### 2.5. Characterization of material properties

Since the mechanical characterization experiments are performed with a thin cylindrical probe on the livers having large surface, it is not possible to obtain hyper-viscoelastic material properties directly from the measurements. For this reason, first, a FE model of liver (Fig. 4) is constructed in ANSYS from axisymmetric 2D elements having homogeneous, isotropic, hyper-viscoelastic, and nearly incompressible material properties and then, an inverse FE analysis is performed on the model to extract the material properties of the livers by inputting the measured experimental data (Samur et al., 2007; Gokgol et al., 2012). In order to reduce the number of FE computations, a two-dimensional FE model is preferred over a three-dimensional one, only the region around the contact is considered for the analysis, and the solution is assumed to be symmetric with respect to the axis of loading. The base of the FE mesh is constrained to have zero displacement.

The hyperelastic behavior of the livers is modeled using the polynomial strain energy function with N=2

$$W = C_{10}(I_1-3) + C_{01}(I_2-3) + C_{20}(I_1-3)^2 + C_{11}(I_1-3)(I_2-3) + C_{02}(I_2-3)^2 \quad (1)$$

where, $C_{10}$, $C_{01}$, $C_{20}$, $C_{11}$ and $C_{02}$ are the material coefficients, and $I_1$ and $I_2$ are the invariants of the left Cauchy-Green deformation tensor.

A Generalized Maxwell Solid (GMS) is used to model the viscoelastic behavior of the livers (Ocal et al., 2010). Then, the time-dependent relaxation of the livers under ramp-and-hold strain input can be expressed analytically as

$$E_R(t) = E_0\left[1 - \sum_{j=1}^{N}\alpha_j\right] + E_0\sum_{j=1}^{N}\alpha_j e^{-t/\tau_j} \quad (2)$$

where, $E_0$ is the short-term elastic modulus, $\alpha_j$ represents the relative modulus, $\tau_j$ stands for the time constant, and $N$ is the number of Maxwell arms used in the GMS model.

The hyperelastic material coefficients ($C_{10}$, $C_{01}$, $C_{20}$, $C_{11}$ and $C_{02}$) and the viscoelastic material coefficients for $N=3$ ($\alpha_1$, $\tau_1$, $\alpha_2$, $\tau_2$, $\alpha_3$, and $\tau_3$) are determined by the inverse FE analysis in

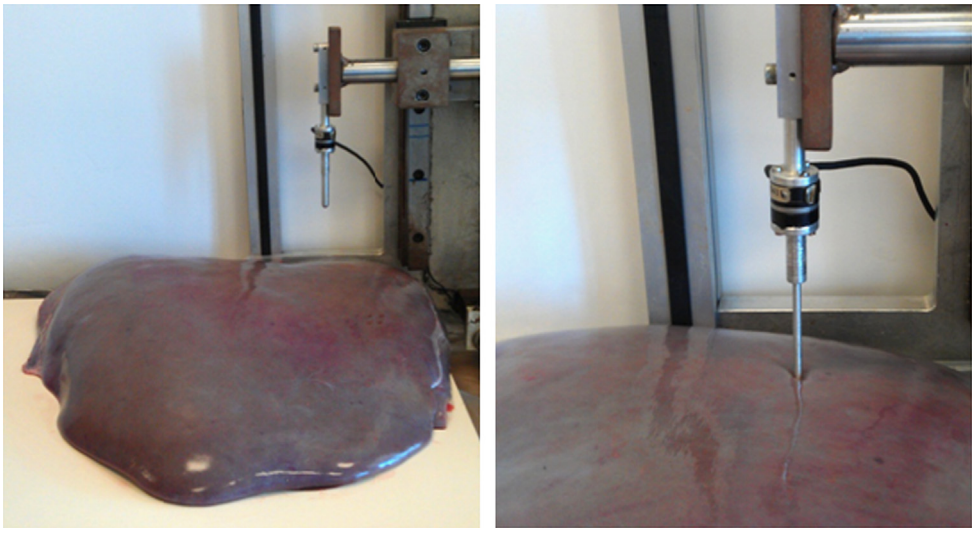

**Fig. 3 – Scenes from the compression experiments performed on one of the livers tested in our study.**

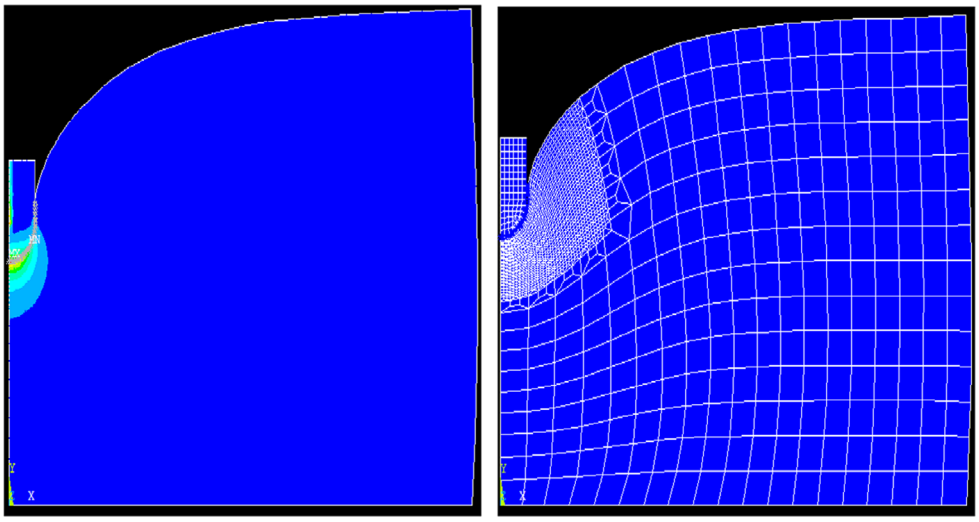

**Fig. 4 – A finite element model of bovine liver deformed with a cylindrical probe.**

ANSYS through optimization iterations (Samur et al., 2007, Gokgol et al., 2012). The optimization algorithm minimizes the force error defined as

$$\text{Error} = \sum_{j=1}^{M} (F_j^{EXP} - F_j^{FEM})^2 \tag{3}$$

where, $M$ represents the number of data samples taken to represent the force curves, $F_j^{EXP}$ is the experimental force value of the $j$th sample, and $F_j^{FEM}$ is the force value obtained from the FE solution at the corresponding time step. The inverse solution is iterated until the total error in force response is less than 0.1 N.

The fracture toughness of each bovine liver is calculated using the energy-based fracture mechanics approach. The data (force versus penetration depth) is collected via two consecutive needle insertions (Gokgol et al., 2012). The energy balance for the first insertion is

$$F_1 du = J dA + d\Delta + P du \tag{4}$$

where, $F_1$ is the force acting on the needle during the first insertion, $du$ is the change in the needle displacement, $J$ is the fracture toughness (material property), $dA$ is the change in crack area, $JdA$ is the fracture work, $d\Delta$ is the change in strain energy, $P$ is the frictional force and $Pdu$ is the work done by the friction. During the second insertion, the needle is inserted to the same spot and no rupture occurs. Hence, the energy balance for the second insertion is

$$F_2 du = d\Delta + P du \tag{5}$$

where, $F_2$ is the force acting on the needle during the second insertion, which is less than $F_1$. The change in strain energy, $d\Delta$, and the work done by the friction, Pdu, are the same for the both insertions.

The fracture toughness, $J$, is obtained by subtracting Eq. (5) from Eq. (4) as

$$J = \int (F_1 - F_2) du \Big/ \int dA \tag{6}$$

### 2.6. *Histological examination*

Histological specimens are prepared from the parenchyma of the caudate lobe of each liver. Small tissue blocks, 3 mm in thickness, are obtained from each liver at different preservation periods for histological examination. The samples are fixed in 10% neutral buffered formalin for 24 h at room temperature to preserve their structure. After the fixation, the samples are dehydrated by bathing them in a graded series of mixtures of ethanol and water. This is followed by a hydrophobic clearing agent (xylene) to remove the alcohol, and finally the infiltration agent (paraffin wax), which replaces the xylene. Then, the samples are heated in the oven at 60 °C for 2 h. Finally, tissue samples are embedded in paraffin. Samples from each specimen are sectioned at 7–10 μm in thickness using a microtome (Leica M72S).

The sections are stained with three different stains for the histological examination: (1) Hematoxylene (Hematoxylene solution modified to Gill III, Merck) and Eosin (Eosin Y solution 0.5% alcoholic, Merck Inc.) (H&E) is utilized for the detection of the structural changes in sinusoids, (2) Masson's trichrome stain (Masson-Goldner Staining kit, Merck Inc.) is utilized to detect the changes in connective tissue and to investigate collagen accumulation, and (3) Periodic-Acid Schiff stain (PAS Staining Kit, Merck Inc.) is utilized to visualize the changes in glycogen deposition in the cytoplasm of the liver cells.

Additionally, hepatocytes, which are undergoing apoptosis, are examined by Apop Tag Plus Peroxidase Kit (Intergen S7101, Millipore Inc.). This kit helps to determine DNA fragmentation in the cells, by labeling the terminal end of nucleic acids, which is known as the TUNEL (Terminal deoxynucleotidyl transferase dUTP nick end labeling) technique.

All treated sections are examined under a light microscope (Axio Imager, Carl Zeiss Inc.). The microscopic images are captured from ten different areas on each section at 100 × magnification. Four software scripts are designed in AxioVision image analysis software (Carl Zeiss Inc.) for the analysis. These scripts enable us (1) to count the nuclei of apoptotic cells (stained as brown/dark brown with Apo Tag Plus

Peroxidase Kit), (2) to measure the accumulation of collagen on each section stained with Masson's trichrome, (3) to measure the area of sinusoids on each section stained with H&E, and (4) the amount of glycogen deposition in the cells on each section stained with PAS.

## 3. Results

### 3.1. Material properties

The average force response of the livers as a function of the compression depth are plotted in Fig. 5A for different preservation periods. The hyperelastic material coefficients of the livers ($C_{10}$, $C_{01}$, $C_{20}$, $C_{11}$, and $C_{02}$) estimated through the inverse FE solution are tabulated in Table 1. The linear elastic modulus (Young's modulus) of the livers for small strain (the last column in Table 1) is calculated by $E = 6(C_{10} + C_{01})$. The change in the linear elastic modulus as a function of preservation period is shown in Fig. 5B.

The viscoelastic material coefficients of the livers ($\alpha_1$, $\tau_1$, $\alpha_2$, $\tau_2$, $\alpha_3$, and $\tau_3$) estimated through the inverse FE solution are tabulated in Table 2. The settling time of the force response is estimated from the relaxation curve by defining a percent relative error as $RE = 100(F_R(t) - F_\infty)/F_\infty$. The relative error is chosen as $RE = 5\%$. The normalized force relaxation response of the bovine livers and the change in settling time as a function of the preservation period are shown in Fig. 6.

The fracture toughness ($J$) of each liver is estimated from the data collected by two consecutive needle insertions. The force displacement responses of the liver of Animal #1 during

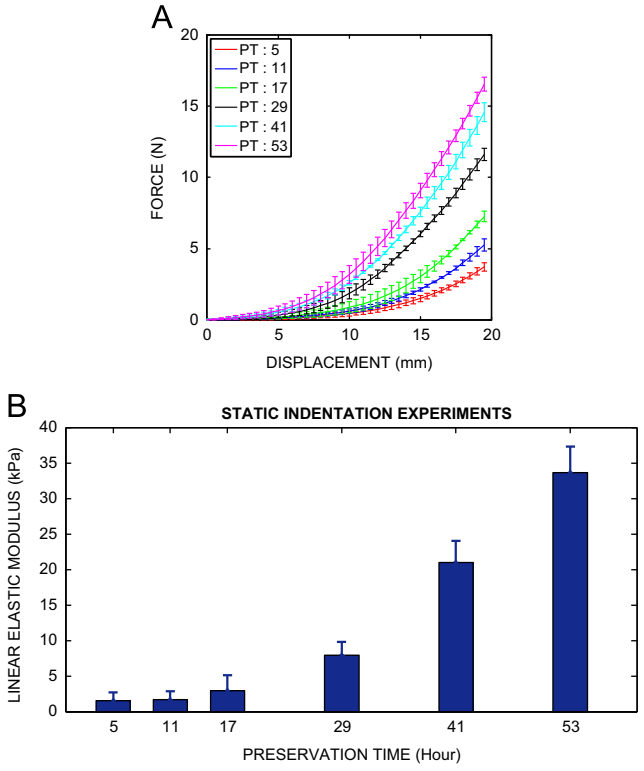


**Fig. 5 – (A) The force response of bovine liver (average of three animals) as a function of compression depth for different preservation times. (B) The linear elastic modulus of bovine liver (average of three animals) as a function of preservation time.**

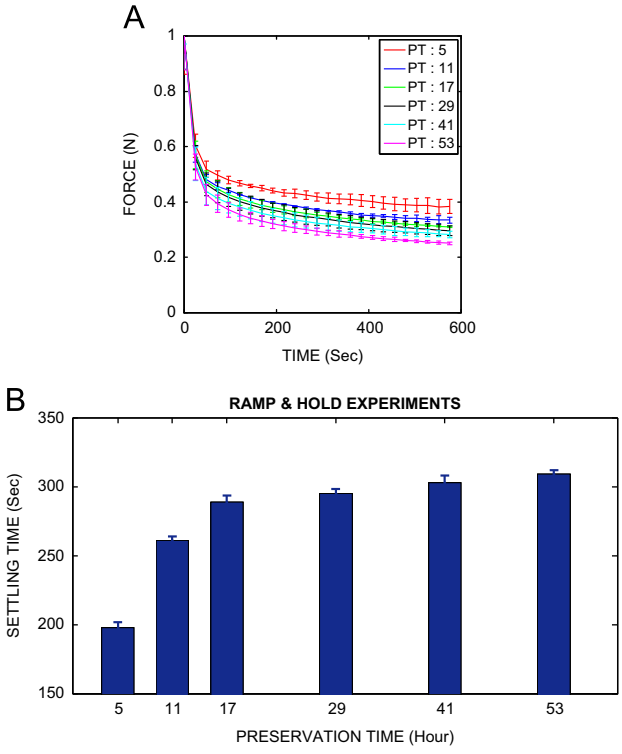


**Fig. 6 – (A) The normalized force relaxation response of bovine liver (average of three animals) for different preservation times. (B) The settling time of the relaxation response for different preservation times.**

**Table 1 – The hyperelastic material coefficients and the linear elastic modulus of bovine liver (average of three animals) for different preservation periods.**

| Preservation time (PT) [h] | $C_{10}$ | $C_{01}$ | $C_{20}$ | $C_{11}$ | $C_{02}$ | Linear elastic modulus, $E$ [kPa] |
|---|---|---|---|---|---|---|
| 5 | 130.8±65.5 | 130.2±47.4 | 200.9±78.6 | 387.1±38.5 | 440.3±148.7 | 1.57±1.1 |
| 11 | 86.9±39.1 | 196.4±97 | 1063.3±66.5 | 252.3±194.3 | 584.6±103 | 1.70±1.1 |
| 17 | 447.7±250.5 | 44.1±22.1 | 1452.7±312.7 | 413.8±141.9 | 706.8±155.9 | 2.95±2.2 |
| 29 | 364.1±78.4 | 953.5±167.3 | 1001.8±218.2 | 1004.0±284.6 | 1061.0±261.6 | 7.91±1.8 |
| 41 | 2100.3±92.1 | 1391.7±206.9 | 725.8±84 | 799.8±125.1 | 579.1±196.1 | 20.95±2.9 |
| 53 | 4435.2±263.3 | 1165.6±488.5 | 72.2±32.4 | 489.4±92.6 | 606.0±184.2 | 33.60±3.7 |

**Table 2 – The viscoelastic material coefficients and settling time of bovine liver (average of three animals) for different preservation periods.**

| Preservation time (PT) [h] | $a_1$ | $a_2$ | $a_3$ | $\tau_1$ | $\tau_2$ | $\tau_3$ | Settling time (ST) [s] |
|---|---|---|---|---|---|---|---|
| 5 | 0.44±0.03 | 0.07±0.01 | 0.28±0.02 | 6.65±0.41 | 37.10±3.75 | 58.80±6.32 | 198±3.8 |
| 11 | 0.42±0.04 | 0.08±0.02 | 0.36±0.03 | 6.74±0.77 | 46.65±4.64 | 64.83±1.50 | 261±2.7 |
| 17 | 0.40±0.02 | 0.08±0.01 | 0.39±0.02 | 6.75±1.46 | 58.63±5.08 | 66.39±2.20 | 289±4.6 |
| 29 | 0.37±0.04 | 0.08±0.02 | 0.37±0.03 | 6.45±1.22 | 65.29±10.1 | 76.18±5.87 | 295±3.2 |
| 41 | 0.32±0.01 | 0.06±0.01 | 0.38±0.09 | 6.95±0.47 | 68.16±7.8 | 84.23±3.52 | 303±5.1 |
| 53 | 0.30±0.06 | 0.08±0.01 | 0.37±0.06 | 5.70±0.62 | 54.87±9.2 | 87.93±12.53 | 309±2.9 |

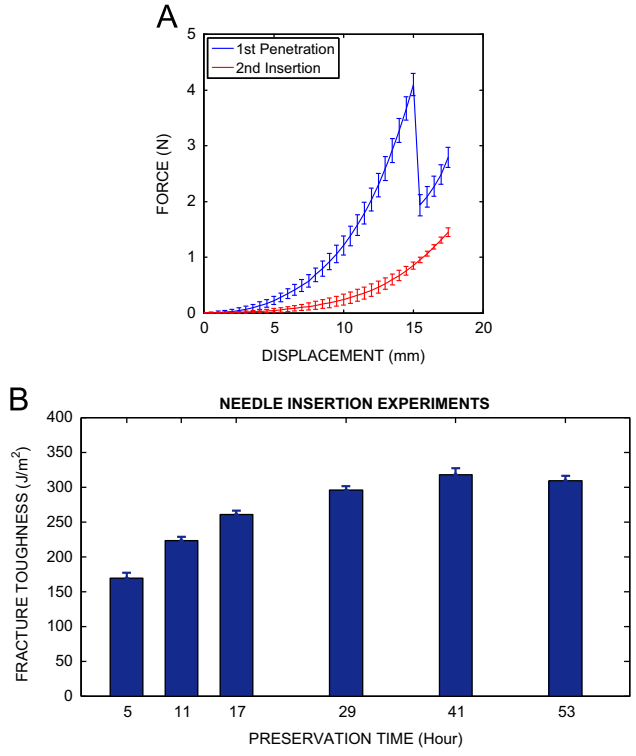


**Fig. 7 – (A) The force displacement responses of the bovine liver of Animal #1 during the first and second needle insertions. (B) The change in fracture toughness of bovine liver (average of three animals) as a function of preservation time.**

the first and second needle insertions are shown in Fig. 7A. As shown in the figure, the curves are parallel after the initial rupture (see the sudden drop in force response in Fig. 7A). The fracture toughness of the liver is estimated by first integrating this difference over the needle displacement and then dividing it by the crack area (the circumference of the probe times the penetration depth). The change in fracture toughness of the bovine livers as a function of preservation period is plotted in Fig. 7B.

### 3.2. *Histological properties*

The changes in histological properties of the bovine livers as a function of preservation period are tabulated in Table 3.

The exemplar images of the tissue sections stained by the TUNEL technique (brown/dark brown) are shown in Fig. 8A and C for PT=5 h and 53 h respectively, and the corresponding images showing the cells marked on micrographs are shown in Fig. 8B and D. The apoptotic cells are counted at 10 different areas on each tissue section. The change in the number of apoptotic cells of the bovine livers as a function of preservation period is plotted in Fig. 8E.

The examination of the sections stained with Masson's trichrome reveals that connective tissue increases as a function of preservation time (Fig. 9A and C). Using the image analysis software, the total area of connective tissue (green colored) on each tissue section is measured (Fig. 9B and D). The change in the connective tissue (especially, the collagen) of the bovine livers as a function of preservation period is plotted in Fig. 9E.

The examination of the sections stained with H&E (outlined with red color) reveals that sinusoidal dilatation is observable only in some areas (Fig. 10A and C). Using the image analysis software, the borders of the sinusoids are outlined first, and then the areas enclosed by these borders are measured (Fig. 10B and D). The change in the sinusoidal dilatation of the bovine livers as a function of preservation time is plotted in Fig. 10E.

The glycogen level in the liver cells has been investigated with the help of PAS stain. As shown in Fig. 11, the glycogen level in the cytoplasm of the cells preserved for PT=53 h (Fig. 11C) is significantly lower than that of PT=5 h (Fig. 11A). The image analysis software labels blue-magenta stained regions on these sections first and then calculates their areas (Fig. 11B and D). The change in the deposited glycogen level in the cells of the bovine livers as a function of preservation period is plotted in Fig. 11E.

Following the characterization of material and histological properties, the correlation between them is investigated via the Spearman's Rank-Order Correlation method. Spearman's Rank-Order Correlation is a measure of a monotonic relationship between two data sets. The significance level is chosen as $p=0.05$. The correlation coefficients, $r_s$, and the strength of the correlation between mechanical and histological properties are presented in Table 4.

Moreover, a sensitivity analysis is performed on the mechanical and histological properties of the liver to determine the upper limit for the preservation period based on the largest change in each property per unit change in preservation time (Table 5). Hence, a normalized sensitivity measure is defined as the change in mechanical/histological property

**Table 3 – The histological properties of bovine liver (average of three animals) for different preservation periods.**

| Preservation time (PT) [h] | Apoptotic cell (AC) [Count] | Fiber tissue (FT) [%] | Sinusoidal dilatation (SD) [%] | Glycogen deposition (GD) [%] |
|---|---|---|---|---|
| 5 | 12.93±6 | 6.17±2.8 | 28.34±13.2 | 35.99±7.9 |
| 11 | 25.5±14.2 | 6.5±2.9 | 30.82±11 | 25.14±9.8 |
| 17 | 36.96±11 | 10.15±4.5 | 30.34±5.9 | 13.88±9.4 |
| 29 | 47.53±13.1 | 14.22±6.7 | 37.1±13.2 | 10.48±8.4 |
| 41 | 44.43±12.2 | 15.29±7.6 | 32.33±5.6 | 8.1±7.63 |
| 53 | 43.96±9.3 | 15.98±6.3 | 38.92±6.6 | 3.31±1.9 |

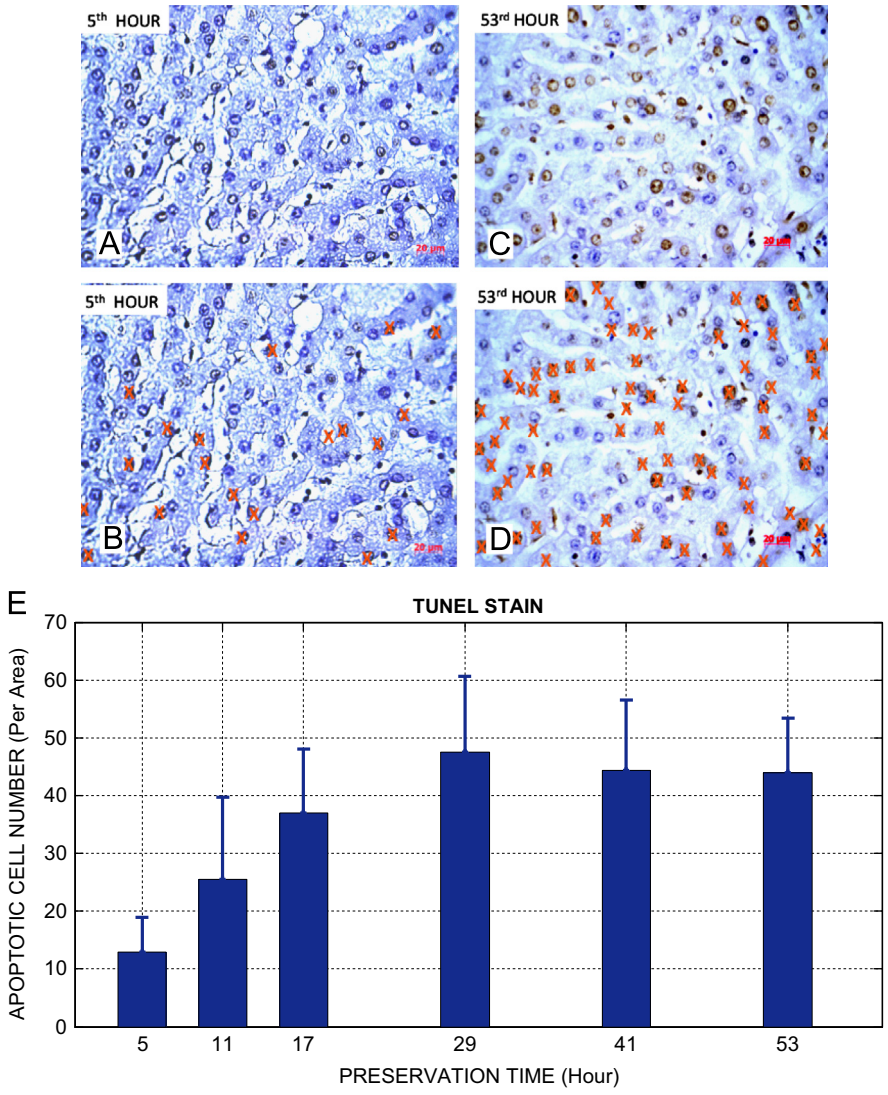


**Fig. 8 – (A, C) The exemplar images of the sections labeled with TUNEL technique and preserved for PT=5 h and PT=53 h. The dark blue stained nuclei shows the healthy cells while the brown/dark brown stained nuclei shows the cells undergoing apoptosis. (B, D) These cells were marked on the micrographs with a cross sign and counted. (E) The change in the apoptotic cell count (average of three animals) as a function of preservation time.**

per change in preservation period.

$$\text{Sensitivity} = 100\frac{(property[k+1]-property[k])/property[k]}{(PT[k+1]-PT[k])} \quad (7)$$

where, '*property*[*k*]' is the *k*th value of a mechanical/histological property measured at '*PT*[*k*]'.

## 4. Discussion

The mechanical properties (stiffness, viscosity, and fracture resistance) of bovine liver increase as a function of preservation period and there is a '*very strong*' correlation among the

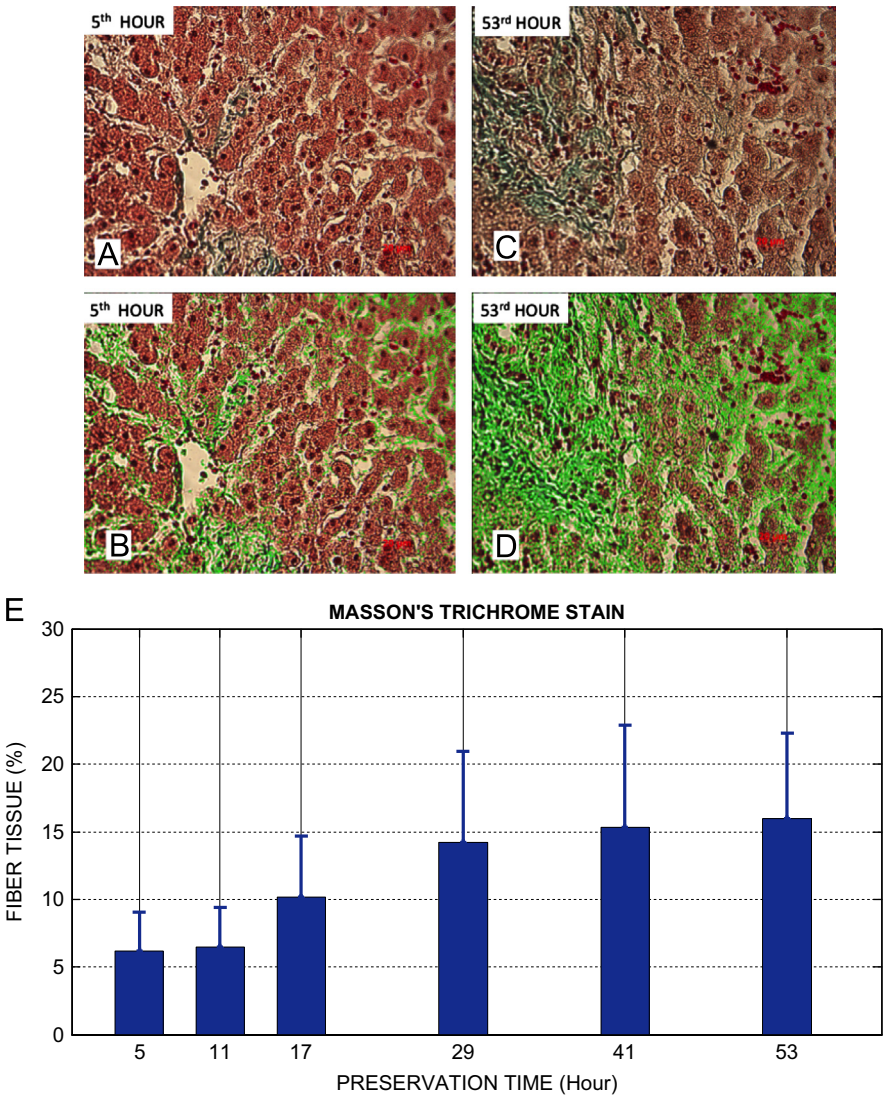


**Fig. 9 – (A, C) The exemplar images of the sections treated by the Masson's trichrome stain and preserved for PT=5 h and PT=53 h. (B, D) The image analysis software measures the areas of green colored regions. (E) The change in the connective tissue (average of three animals) as a function of preservation time.**

properties (Table 4). The results of the static indentation experiments performed in this study show that the liver tissue becomes stiffer as it spends more time in the preservation solution. We observed that the tangent elastic modulus of bovine liver varies between 1.6 kPa (PT=5 h) and 33.6 kPa (PT=53 h). Hence, our results suggest that bovine liver preserved in Lactated Ringer solution for 53 h becomes almost 21 times stiffer than that of 5 h ($p<0.05$). All these values are in line with the earlier findings in the literature. Chen et al. (1996) estimated the elastic modulus of bovine liver between 0.4 and 0.7 kPa using an ultrasound device and between 0.3 and 1.6 kPa using a mechanical tensile testing device. Ocal et al. (2010) estimated the elastic modulus of fresh bovine liver as 4.1 kPa. Liu and Bilston (2000) performed rheological experiments and reported the shear modulus of bovine liver as 0.6 kPa. Brosses et al. (2010) examined the material properties of bovine liver using the Supersonic Shear Imaging (SSI) technique and estimated its shear modulus as 3.4 kPa. The linear elastic modulus of porcine liver was estimated as ~10 kPa in the earlier studies (Kruse et al., 2000; Ottensmeyer, 2001; Samur et al., 2005; Tay et al., 2006). The elastic modulus of human liver was estimated as ~20 kPa by Nava et al. (2008) and between 10 and 20 kPa by Ozcan et al. (2011).

The results of our ramp and hold experiments show that the liver tissue becomes more viscous as it spends more time in the preservation solution, which is in agreement with the results of the earlier studies (Kerdok et al., 2006; Ocal et al., 2010). As the tissue becomes more viscous, it takes longer for it to relax and reach steady state, as shown in Fig. 6A. Our results (Fig. 6B) suggest that bovine tissue preserved for 53 h becomes 1.6 times more viscous than that of 5 h ($p<0.05$).

The results of the needle insertion experiments show that the fracture toughness of the liver increases up to PT=29 h, but no significant change is observed after that. We found that the toughness values vary between $169\pm7$ J/m$^2$ (PT=5 h) and $308\pm6$ J/m$^2$ (PT=53 h). Hence, our results suggest that it

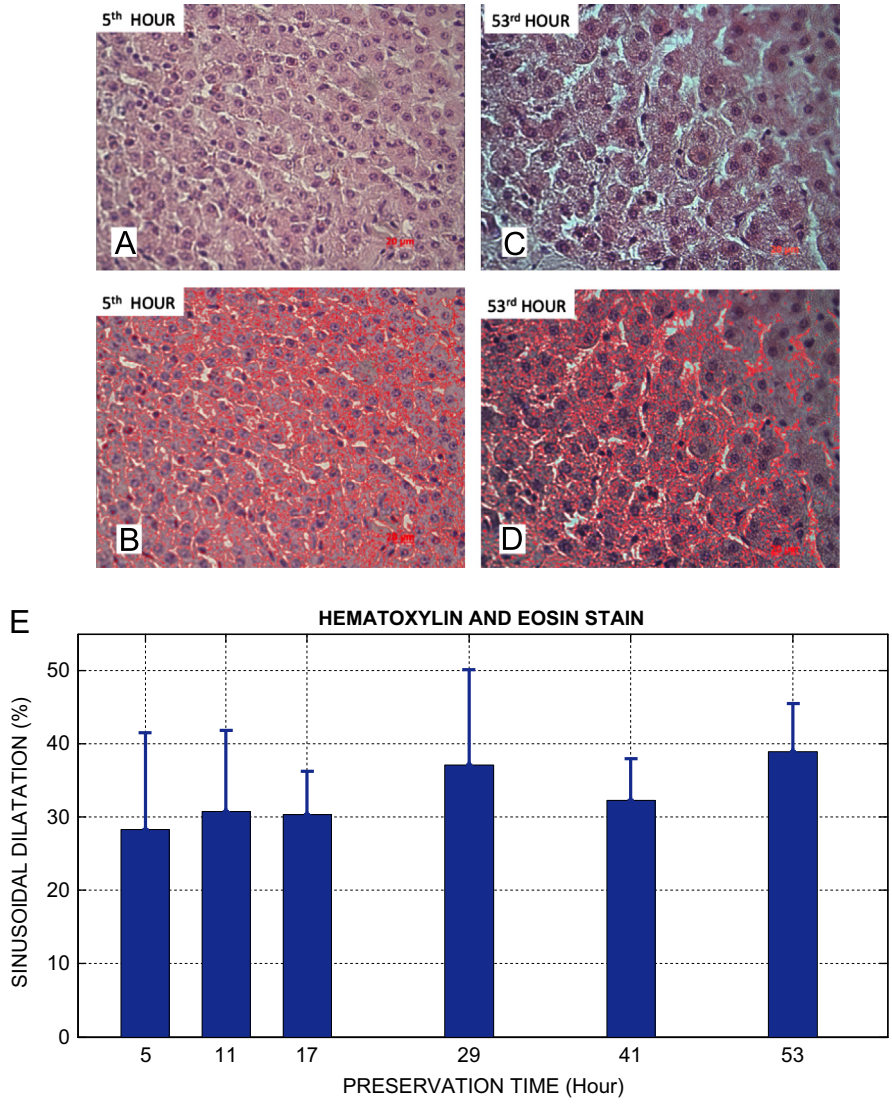


**Fig. 10 – (A, C) The microphotographs show the sections stained with the Hematoxylene and Eosin and preserved for PT = 5 h and PT = 53 h. (B, D) The marked areas show the dilated sinusoids. (E) The change in the sinusoidal dilatation (average of three animals) as a function of preservation time.**

is 1.8 times more difficult to cut or tear bovine liver tissue preserved for 53 h, compared to the one preserved for 5 h ($p<0.05$). These results are in good agreement with the earlier findings. Gokgol et al. (2012) estimated the fracture toughness of bovine liver as $164\pm6$ J/m$^2$. The fracture toughness of porcine liver was estimated to vary between 75.8 J/m$^2$ and 185.6 J/m$^2$ in Azar and Hayward (2008) and between 186.9 and 224.8 J/m$^2$ in Chanthasopeephan et al. (2006).

In the histological examination, the changes in apoptotic cell count, collagen accumulation, sinusoidal dilatation and glycogen deposition in hepatocytes are investigated as a function of preservation period. Our results show ~4-folds increase in apoptotic cell count at PT = 29 h compared to PT = 5 h ($p<0.05$), but no significant change is observed after PT = 29 h ($p>0.05$). Natori et al. (1999) investigated the apoptosis of sinusoidal endothelial cells during cold preservation of liver. The results showed that the number of apoptotic cells have increased 6-folds after 24 h of preservation. Toom et al. (1991) investigated the effects of preservation solutions on the morphology of rat liver. They observed a significant morphological damage in liver cells preserved for 42 h compared to 18 h. Apoptosis is also linked to the disease progression in the literature. Malhi et al. (2006) suggested that apoptosis is a prominent factor of chronic liver diseases. It has also been reported that apoptosis stimulates inflammatory and fibrotic changes (Canbay et al. 2004). Calabrese et al. (2000), investigated the apoptotic cell levels in hepatitis C virus (HCV) infection, and they found that the apoptotic cell index varies between 0.01% and 0.54% and the index increases with the level of infection.

Our results show that the accumulation of fibrous tissue at PT = 29 h is ~2.5 times higher than the value measured at PT = 5 h ($p<0.05$), but no significant change is observed after PT = 29 h ($p>0.05$). There is '*very strong*' correlation (Table 5) between the apoptotic cell count and the accumulation of fibrous tissue since the decrease in blood supply naturally triggers the programmed cell death and this controlled

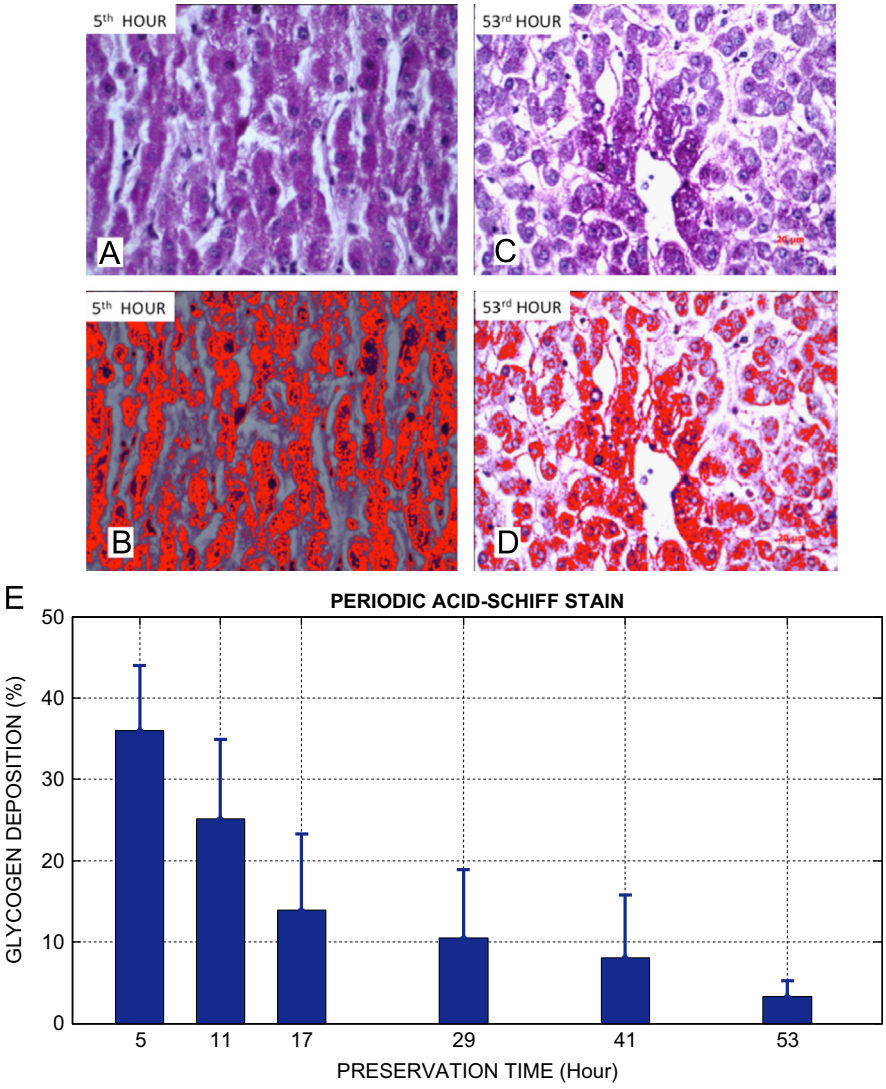


**Fig. 11 – (A, C) The exemplar images of the sections stained with the Periodic Acid-Schiff and preserved for PT = 5 h and PT = 53 h. (B, D) The image analysis software measures the magenta colored regions. (E) The change in the deposited glycogen level (average of three animals) as a function of preservation time.**

**Table 4 – The correlation coefficients, $r_s$, and the strength of correlation (0–0.19: 'very weak', 0.20–0.39: 'weak', 0.40–0.59: 'moderate', 0.60–0.79: 'strong', 0.80–1.0: 'very strong'; SI: statistically insignificant) between the mechanical and histological properties of bovine liver.**

| Correlation coefficient ($r_s$) | Apoptotic cell count | Connective tissue | Sinusoidal dilatation | Glycogen deposition | Young's modulus | Fracture toughness | Settling time |
|---|---|---|---|---|---|---|---|
| Apoptotic cell count | – | 0.84 | SI | −0.48 | 0.51 | 0.68 | 0.69 |
| Connective tissue | *Very strong* | – | SI | −0.66 | 0.74 | 0.80 | 0.83 |
| Sinusoidal dilatation | SI | SI | – | −0.53 | SI | SI | SI |
| Glycogen deposition | *Moderate* | *Strong* | *Moderate* | – | −0.90 | −0.92 | −0.87 |
| Young's modulus | *Moderate* | *Strong* | SI | *Very strong* | – | 0.87 | 0.81 |
| Fracture toughness | *Strong* | *Very strong* | SI | *Very strong* | *Very strong* | – | 0.90 |
| Settling time | *Strong* | *Very strong* | SI | *Very strong* | *Very strong* | *Very strong* | – |

**Table 5 – The sensitivity values calculated for the histological and mechanical properties.**

| Preservation time (PT) | Apoptotic cell count | Connective tissue | Sinusoidal dilatation | Glycogen deposition | Young's modulus | Fracture toughness | Settling time |
|---|---|---|---|---|---|---|---|
| 5 | – | – | – | – | – | – | – |
| 11 | 16.19±1.75 | 0.87±0.09 | 1.46±0.16 | −5.01±0.55 | 1.49±0.16 | 10.76±1.19 | 5.30±0.58 |
| 17 | 7.49±0.83 | 9.35±1.03 | −0.26±0.02 | −7.46±0.82 | 12.26±1.36 | 4.64±0.51 | 1.78±0.19 |
| 29 | 2.38±0.26 | 3.34±0.37 | 1.85±0.2 | −2.04±0.22 | 13.98±1.55 | 1.68±0.18 | 0.14±0.01 |
| 41 | −0.54±0.06 | 0.58±0.06 | −1.07±0.11 | −1.89±0.21 | 13.75±1.24 | 0.86±0.09 | 0.25±0.02 |
| 53 | −0.08±0 | 0.41±0.04 | 1.7±0.18 | −4.92±0.54 | 5.03±0.55 | −0.31±0.03 | 0.16±0.01 |

mechanism also involves the cells which produce connective tissue.

Our results show a slight increase in sinusoidal dilatation as a function of preservation time, but the results are not statistically significant. Jain et al. (2004) and Puhl et al. (2006) investigated the change in sinusoidal dilatation levels during cold storage and perfusion and observed an increase in sinusoidal dilatation as a function of preservation period due to perfusion damage.

Our results show a significant decrease (10 folds) in the glycogen level when the value measured at PT=5 h is compared to the one measured at PT=5 h ($p<0.05$), which has a '*moderate*' negative correlation with the apoptotic cell count and a '*strong*' negative correlation with the accumulated connective tissue (Table 5). The glycogen is made and stored primarily in the liver cells, and functions as the secondary energy storage. This result shows that certain percentage of hepatocytes could not synthesize and store glycogen since the deposited glycogen was consumed for the survival and then the cells underwent to apoptosis. Corps et al. (2009) investigated the cell viability in rat livers with different preservation solutions during cold ischemia. ATP, ADP and AMP degraded in 4 h and the results showed a significant decrease in the glycogen levels. Nowak et al. (2002) and Zaouali et al. (2010) investigated energy kinetics and glycogen-ATP contents and observed a decrease in glycogen levels as a function of preservation period.

Table 5 shows that there is a strong relation between the mechanical and histological properties of the bovine liver. The mechanical properties (stiffness, viscosity, and fracture resistance) are strongly correlated with apoptotic cell count (positive), very strongly with the connective tissue (positive) and the glycogen level (negative), and not correlated at all to the sinusoidal dilation. These results are also in agreement with the results of the earlier studies, which are limited in number. The correlation between the fibrous tissue and liver stiffness has been already reported (Sandrin et al., 2003; Ziol et al., 2005; Manduca et al., 2001; Huwart et al., 2006; Mazza et al., 2007; Ozcan et al., 2011). Mori et al. (2011) investigated the correlation between liver stiffness and collagen accumulation with patients who have non-alcoholic fatty liver disease. They observed that not only the increase in the collagen level, but also the presence of myofibroblasts triggers the chronic liver diseases. Leal-Egaña et al. (2012) investigated the effect of fibrous structure on the spread of liver cancer, and the mechanical property of liver. They suggest that the progression of liver cancer can be prevented by tuning the stiffness of liver. Lake and Barocas (2012)investigated the effect of the initial collagen alignment on the mechanical properties of soft tissues. The results showed that different initial alignments do not directly affect the strain-dependent elastic response, but have an influence on the time-dependent relaxation response.

Investigating the relation between mechanical and histological properties not only provides insight into liver damage during disease progression but also during liver preservation for transplantation. During the liver transplantation, the donor and the recipient are mostly in different locations, so the preservation conditions and the transportation duration are both very important. Preservation solutions are designed to inhibit the negative effects of ischemia and to maintain the tissue viability. However, even the most effective solutions can preserve the organ up to certain duration only, though there is no consensus among the physicians on how long this period should be. In this study, we investigated the change in material and histological properties of bovine liver during cold storage. The sensitivity analysis showed that the largest changes in mechanical and histological properties occur between 11 and 17 h. Although the largest change in liver stiffness was observed after 17 h of preservation, the largest changes in viscosity and fracture toughness occurred after 11 h of preservation. The largest change in apoptotic cell count occurred after 11 h, and for collagen accumulation and glycogen deposition, the largest changes were observed after the first 17 h.

## 5. Conclusion

In order to better understand the damage occurring in liver tissue during disease progression and preservation, the relation between the mechanical and histological properties of liver must be investigated in depth. However, the number of studies in the literature investigating the relationship between the mechanical and histological properties of liver is very limited. Most of the earlier studies in this area have focused on the measurement of one mechanical property (elastic modulus) at a certain frequency, and then finding its correlation with semi-quantitative histological scores. We suggest that the liver damage during disease progression (or during liver preservation) can only be understood truly if the relation between the states of mechanical and histological properties is investigated as a function of time as it is done in dynamical systems theory to investigate the behavior of complex systems. Our results show that stiffness, viscosity and fracture toughness of the bovine livers increase as a

function of preservation time. Moreover, the number of apoptotic cells and the connective tissue around cells increase while the glycogen level decrease as the liver spends more time in the preservation solution. Finally, the changes in stiffness, viscosity and fracture toughness of the livers are strongly correlated with the changes in the accumulated connective tissue (positive) and the glycogen level (negative).

In addition to investigating the mechanical and histological properties of liver tissue and the correlations between them, our study also provides insight into how long the liver should be preserved in a Lactated Ringer solution. Our results show that the largest changes in mechanical and histological properties occur after the first 11–17 h of preservation. With the insight gained in this study, we plan to further investigate the effect of commonly used preservation solutions in liver transplantation (University of Wisconsin and HTK) on the mechanical and histological properties of the liver harvested from a donor. Additionally, we plan to examine liver samples under an electron microscope. Through this examination, more insight can be gained about the changes occurring at molecular level in intracellular matrix (ICM).

## REFERENCES


Azar, T., Hayward, T., 2008. Estimation of the fracture toughness of soft tissue from needle insertion. In: Proceedings of the 4th International Symposium on Biomedical Simulations (ISBMS), pp. 166–175.

Battaler, R., Brenner, D.A., 2005. Liver fibrosis. Journal of Clinical Investigation 115, 209–218.

Brosses, E.S., Gennison, J.L., Pernot, M., Fink, M., Tanter, M., 2010. Temperature dependence of the shear modulus of soft tissues assessed by ultrasound. Physics in Medicine and Biology 55, 1701–1718.

Calabrese, F., Pontisso, P., Pettenazzo, E., Benvegnu, L., Vario, A., Chemello, L., Alberti, A., Valente, M., 2000. Liver cell apoptosis in chronic hepatitis C correlates with histological but not biochemical activity or serum HCV-RNA levels. Hepatology 31, 1153–1159.

Canbay, A., Freidman, S., Gores, G.J., 2004. Apoptosis: the nexus of liver injury and fibrosis. Hepatology 39, 273–278.

Chanthasopeephan, T., Desai, J.P., Lau, A.C.W., 2006. Determining fracture characteristics in scalpel cutting of soft tissue. In: Proceedings of IEEE/RAS-EMBS Conference on Biomedical Robotics and Biomechatronics, pp. 899–904.

Chen, E.J., Novakofski, J., Jenkins, W.K., O'Brien, W.D., 1996. Young's modulus measurements of soft tissues with application to elasticity imaging. IEEE Transactions on Ultrasonics Ferroelectrics and Frequency Control 43, 191–194.

Cui, D.X., Yin, J.Q., Xu, W.X., Chai, F., Liu, B.L., Zhang, X.B., 2010. Effects of different bile duct flush solutions on biliary tract preservation injury of donated livers for transplantation. Transplantation Proceedings 42, 1576–1581.

Corps, C.L., Shires, M., Crellin, D., Smolenski, R., Potts, D., Pratt, J., Lodge, J.P.A., 2009. Influence on energy kinetics and histology of different preservation solutions seen during cold ischemia in the liver. Transplantation Proceedings 41, 4088–4093.

Gokgol, C., Basdogan, C., Canadinc, D., 2012. Estimation of fracture toughness of liver tissue: experiments and validation. Medical Engineering and Physics 34, 882–891.

Guibert, E.E., Petrenko, A.Y., Balaban, C.L., Somov, A.Y., Rodriguez, J.V., Fuller, B.J., 2011. Organ preservation: current concepts and new strategies for the next decade. Transfusion Medicine and Hemotherapy 38, 125–142.

Huwart, L., Peeters, F., Sinkus, R., Annet, L., Salameh, N., ter Beek, L.C., Horsmans, Y., Van Beers, B.E., 2006. Liver fibrosis: non-invasive assessment with MR elastography. NMR in Biomedicine 19, 173–179.

Jain, S., Xu, H., Duncan, H., Jones Jr., J.W., Zhang, J.X., Clemens, M.G., Lee, C.Y., 2004. Ex-vivo study of flow dynamics and endothelial cell structure during extended hypothermic machine perfusion preservation of livers. Cryobiology 48, 322–332.

Kerdok, A.E., Ottensmeyer, M.P., Howe, R.D., 2006. Effects of perfusion on the viscoelastic characteristics of liver. Journal of Biomechanics 39, 2221–2231.

Kruse, S.A., Smith, J.A., Lawrence, A.J., Dresner, M.A., Manduca, A., Greenleaf, J.F., Ehman, R.L., 2000. Tissue characterization using magnetic resonance elastography: preliminary results. Physics in Medicine and Biology 45, 1579–1590.

Lake, S.P., Barocas, V.H., 2012. Mechanics and kinematics of soft tissue under indentation are determined by the degree of initial collagen fiber alignment. Journal of the Mechanical Behavior of Biomedical Materials 13, 25–35.

Leal-Egaña, A., Fritsch, A., Heidebrecht, F., Díaz-Cuenca, A., Nowicki, M., Bader, A., Käs, J., 2012. Tuning liver stiffness against tumours: an in vitro study using entrapped cells in tumour-like microcapsules. Journal of the Mechanical Behavior of Biomedical Materials 9, 113–121.

Liu, Z., Bilston, L., 2000. On the viscoelastic character of liver tissue: experiments and modeling of the linear behavior. Biorheology 37, 191–201.

Malhi, H., Gores, G.J., Lemasters, J.J., 2006. Apoptosis and necrosis in the liver: a tale of two deaths? Hepatology 43, S31–S44.

Manduca, A., Oliphant, T.E., Dresner, M.A., Mahowald, J.L., Kruse, S.A., Amromin, E., Felmlee, J.P., Greenleaf, J.F., Ehman, R.L., 2001. Magnetic resonance elastography: non-invasive mapping of tissue elasticity. Medical Image Analysis 5, 237–254.

Mazza, E., Nava, A., Hahnloser, D., Jochum, W., Bajka, M., 2007. The mechanical response of human liver and its relation to histology: an in vivo study. Medical Image Analysis 11, 663–672.

Mori, M., Fujii, H., Ogawa, T., Kobayashi, S., Iwai, S., Morikawa, H., Enomoto, M., Tamori, A., Sawada, A., Takeda, S., Kawada, N., 2011. Close correlation of liver stiffness with collagen deposition and presence of myofibroblasts in non-alcoholic fatty liver disease. Hepatology Research 41 (9), 897–903.

Natori, S., Selzner, M., Valentino, K.L., Fritz, L.C., Srinivasan, A., Clavien, P.A., Gores, G.J., 1999. Apoptosis of sinusoidal endothelial cells occurs during liver preservation injury by a caspase-dependent mechanism. Transplantation 68, 89–96.

Nava, A., Mazza, E., Furrer, M., Villiger, P., Reinhart, W.H., 2008. In vivo mechanical characterization of human liver. Medical Image Analysis 12, 203–216.

Nowak, G., Ungerstedt, J., Wernerman, J., Ungerstedt, U., Ericzon, B.G., 2002. Metabolic changes in the liver graft monitored continuously with microdialysis during liver transplantation in a pig model. Liver Transplantation 8, 424–432.

Ocal, S., Ozcan, M.U., Basdogan, I., Basdogan, C., 2010. Effect of preservation period on the viscoelastic material properties of soft tissues with implications for liver transplantation. Journal of Biomechanical Engineering 132 (10), 101007.

Ottensmeyer, M.P., 2001. Minimally invasive instrument for in vivo measurement of solid organ mechanical impedance. Ph.D. Thesis, Department of Mechanical Engineering, MIT.

Ozcan, M.U., Ocal, S., Basdogan, C., Dogusoy, G., Tokat, Y., 2011. Characterization of frequency-dependent material properties of human liver and its pathologies using an impact hammer. Medical Image Analysis 15, 45–52.

Puhl, G., Olschewski, P., Schöning, W., Hunold, G., Liesaus, H.G., Winkler, R., Neumann, U.P., Schubert, T.E.O., Schmitz, V., Neuhaus, P., 2006. Low viscosity histidine-tryptophan-ketoglutarate graft flush improves subsequent extended cold storage in university of wisconsin solution in an extracorporeal rat liver perfusion and rat liver transplantation model. Liver Transplantation 12, 1841–1849.

Rockey, Don C., Caldwell, S.H., Goodman, Z.D., Nelson, R.C., Smith, A.D., 2009. Liver biopsy. Hepatology 49, 1017–1044.

Samur, E., Sedef, M., Basdogan, C., Avtan, L., Duzgun, O., 2005. A robotic indenter for minimally invasive characterization of soft tissues. In: Proceedings of the International Conference on Computer Assisted Radiology and Surgery, vol. 1281, pp. 713–718.

Samur, E., Sedef, M., Basdogan, C., Avtan, L., Duzgun, O., 2007. A robotic indenter for minimally invasive measurement and characterization of soft tissue behavior. Medical Image Analysis 11, 361–373.

Sandrin, L., Fourquet, B., Hasquenoph, J.M., Yon, S., Fournier, C., Mal, F., Christidis, C., Ziol, M., Poulet, B., Kazemi, F., Beaugrand, M., Palau, R., 2003. Transient elastography: a new noninvasive method for assessment of hepatic fibrosis. Ultrasound in Medicine and Biology 29, 1705–1713.

Shiha, G., Zalata, K., 2011. Ishak versus METAVIR: terminology, convertibility and correlation with laboratory changes in chronic hepatitis C. Liver Biopsy 10, 155–170.

Tay, B.K., Kim, J., Srinivasan, M.A., 2006. In vivo mechanical behavior of intra-abdominal organs. IEEE Transactions on Biomedical Engineering 53, 2129–2138.

Toom, R.D., Jong, M.D., Krenning, E.P., Hoek, H.J.V.D., Kate, F.J.W.T., Henneman, G., Terpstra, O.T., 1991. Euro-collins solution versus uw-solution for long-term liver preservation in the isolated rat-liver perfusion model. HPB Surgery 4, 313–320.

Zaouali, M., Padrissa-Altés, S., Ben Mosbah, I., Alfany-Fernandez, I., Massip-Salcedo, M., Casillas-Ramirez, A., Bintanel-Morcillo, M., Boillot, O., Serafin, A., Rimola, A., Rodés, J., Roselló-Catafau, J., Peralta, C., 2010. Improved rat steatotic and nonsteatotic liver preservation by the addition of epidermal growth factor and insulin-like growth factor-I to University of Wisconsin solution. Liver Transplantation 16, 1098–1111.

Ziol, M., Handra-Luca, A., Kettaneh, A., Christidis, C., Mal, F., Kazemi, F., de Ledinghen, V., Marcellin, P., Dhumeaux, D., Trinchet, J.C., Beaugrand, M., 2005. Noninvasive assessment of liver fibrosis by measurement of stiffness in patients with chronic hepatitis CHepatology 41 (1), 48–54.